

Molybdenum and Tungsten Coatings for X-Ray Targets Obtained through the Low-Pressure Plasma Spraying Process

A.A. Khan, J.C. Labbe, A. Grimaud, and P. Fauchais

Low-pressure plasma spraying under an argon atmosphere was employed to deposit molybdenum and tungsten coatings on different metallic, ceramic, and composite substrates. Molybdenum coatings obtained through this technique presented a homogeneous structure with an average porosity of about 17%. These coatings exhibited adhesion greater than 40 MPa on molybdenum and grey cast iron (FT25) substrates. No adhesion was observed on an AlN surface regardless of the preheating temperature and/or surface preparation. Adhesion on AlN-Mo (AM25) composite substrate, containing 25% dispersed metallic phase by volume, showed intermediate results. Tungsten coatings exhibited porosity between 10 to 12% and a typical lamellar structure. The adhesion of tungsten coatings on molybdenum and FT25 substrates was around 40 MPa.

Keywords adhesion, AlN-Mo composite, low-pressure plasma spraying, molybdenum coatings, porosity, tungsten coatings, x-ray target

1. Introduction

COATINGS of tungsten and tungsten-base alloys are frequently employed as targets in high-temperature appliances working under vacuum. One of these applications is high power x-ray tubes used for continuous operation in medical examinations. The anode of such tubes is composed of a tungsten coating that serves as a target, deposited over an appropriate substrate. Target life and working performances are directly related to the properties of the deposited layer (e.g., porosity, microstructure, residual stresses) and to the adhesion between the coating and the substrate (Ref 1). Under-layers are sometimes used to compensate for the differences in thermal expansion coefficient between the target and the substrate. Anode substrates are currently made from graphite. New substrates based on AlN-Mo composites (Ref 1) were studied to improve the mechanical and thermal properties of targets as well as the target life. This work was undertaken to develop and characterize plasma-sprayed tungsten coatings on the desired substrate. Molybdenum coatings were also examined in view of their possible application as an under-layer.

Low-pressure plasma spraying under an argon atmosphere can be successfully applied to the spraying of refractory metals that are reactive to oxygen (Ref 2). Low-pressure spraying, for which the spraying chamber pressure is kept between 15 to 35 kPa, presents many advantages over classical techniques, such as high gas velocities, high preheating temperatures, low porosity, and better adhesion of the coatings. However, heat transfer to the particles is reduced, which renders the melting of refractory metals more difficult than at atmospheric pressure under argon

atmosphere. In this type of spraying process, the sprayed target (sample), plasma torch, and displacement equipment are placed inside a hermetically closed chamber provided with an adequate vacuum pumping system.

This technique was employed to obtain MCrAlY coatings on angular and curved surfaces (Ref 3). Successful attempts were made (Ref 4) to obtain thick-walled, near-theoretical-density tungsten tubing by spraying over the surface of thin-walled tungsten tubes produced by the chemical vapor deposition process, where a postspraying thermal treatment under vacuum improved the density of these tungsten coatings.

Spraying of titanium coatings (Ref 5) under air and low-pressure argon atmosphere has shown that spraying under controlled atmosphere resulted in high density and homogeneous structures, whereas high hardness values were obtained for those projected under air, mainly due to the incorporation of oxide and nitride impurities. Similar results were shown (Ref 6) during the spraying of corrosion resistant stainless steel coatings where coatings produced by low-pressure plasma spraying presented low porosity and better adhesion compared to those produced by atmospheric plasma spraying. Moreau et al. (Ref 7) underlined the importance of the spraying atmosphere on the microstructure and thermal diffusivity of plasma-sprayed tungsten coatings. They found that the absence of oxide impurities at inter-lamellar contacts improved the thermal diffusivity of these coatings.

Successful efforts were also made to produce dense tungsten coatings (Ref 8) through the low-pressure controlled atmosphere ($2 \times 10^4 < p < 4 \times 10^4$ Pa) induction coupled plasma spraying technique. This technique produced good quality coatings up to 95% of their theoretical density. Other works concerning tungsten and molybdenum spraying (Ref 9, 10) mentioned the influence of spraying atmosphere on the quality of sprayed films. McKechnie et al. (Ref 9) obtained high-density partially recrystallized tungsten films through the LPPS technique on substrates preheated at temperatures between 900 to 1150 °C. As well, decarburization of Mo-Mo₂C composite coatings could be considerably reduced (Ref 8) while spraying under controlled atmosphere, due to the low oxygen partial pressure (less than 1 Pa) in the chamber.

A.A. Khan, J.C. Labbe, A. Grimaud, and P. Fauchais, Laboratoire de Matériaux Céramiques et Traitements de Surface, URA CNRS 320, 123 Av. Albert Thomas, Faculté des Sciences, Université de Limoges, 87060 Limoges Cedex, France.

In this work we examined the properties of tungsten and molybdenum films deposited through low-pressure spraying on metallic, ceramic, and composite substrates based on AlN and molybdenum, our goal being to obtain targets used in high-power x-ray tubes employed in medical applications. As discussed earlier, anodes of x-ray tubes are mostly composed of a tungsten target made of a coating over an adequate substrate. New substrate materials are being developed to sustain the severe working conditions of temperatures as high as 1500 °C and high mechanical stresses.

Aluminum nitride/molybdenum ceramic matrix composites (Ref 1) were developed as target substrates and exhibited excellent refractory properties with high mechanical strength. In the present work we studied not only the spraying conditions and coating properties but also the compatibility between a given type of coating and substrates of various nature, with the objective of obtaining the best adhesion between the coating and the substrate.

2. Spraying Technique and Equipment

Figure 1 shows a simplified diagram of the equipment used in low-pressure spraying. A direct current arc plasma generator was placed inside the spraying chamber supplied with a vacuum pumping system. The custom-built plasma gun (identified as Lab. 114) consisted of an anode made of electrolytic copper, 6 mm in internal diameter, and a conical rod-shaped thoriated (2 wt%) tungsten cathode. Powder particles were injected 3 mm upstream of the nozzle exit, into the plasma jet, through a 1.8 mm internal diameter tube. Substrate samples were disc-shaped, 25 mm in diameter and 5 mm in thickness, fixed on a cylindrical sample holder. Rotation of the sample holder was ensured with an electric motor to obtain a sample displacement tangential speed of about 550 mm/s. The plasma gun was moved back and forth over a track parallel to the cylindrical holder axis to achieve a translation movement at a speed of 10 mm/s, to achieve a uniform thickness distribution of the coating.

The resulting bead overlapping was about 50%. Temperature measurements during preheating and spraying were performed using a bichromatic pyrometer coupled with an optical fiber. An initial vacuum of 100 Pa was established inside the spraying chamber before the introduction of argon, and the pressure was

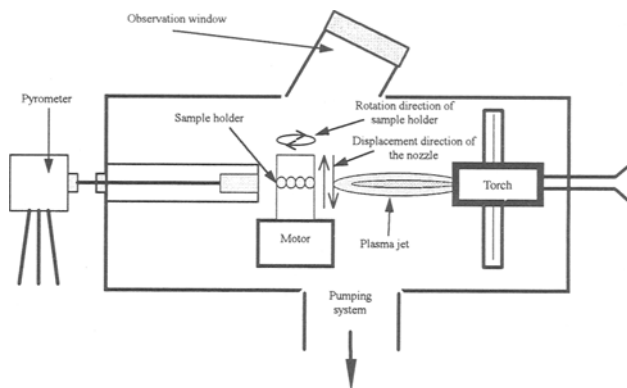


Fig. 1 Simplified diagram of the equipment used in low-pressure plasma spraying

kept around 4×10^4 Pa during the spraying operation. An observation window on the chamber allowed the spraying operation to be followed and anomalies to be detected during spraying. Preheating of the samples was performed by using the plasma torch, under spraying conditions, before the introduction of powder.

3. Description of Powders and Substrates

Two types of spraying powders were employed:

- *Molybdenum powder (Amperit 105-054)* was supplied by C. Starck, Berlin. The powder was agglomerated and sintered with at least 97% grains between 10 and 45 μm (Fig. 2). This powder was composed of quasispherical agglomerated particles obtained through spray drying and sintering. The particle agglomerates appeared to be hollow, which could result in their breakdown during spraying. The powder was 99.88% pure according to the specifications given by the producer, and the oxygen content was less than 0.12%.
- *Tungsten powder (Amperit 140-3)* was produced and supplied by C. Starck, Berlin. This powder had 98.5% particles with sizes between 5 and 45 μm (Fig. 3). The powder particles were composed of dense sintered agglomerates containing a relatively higher quantity of fine particles. Its shape factor being lower than that of molybdenum (0.6 against 0.9), this powder exhibited lower floatability. The shape factor is defined as the ratio between the surface area of a sphere to that of a powder grain particle of the same volume. This problem was increased by the presence of a higher quantity of fine particles. The powder was 99.8% pure with an oxygen content of less than 0.075%.

The different substrate materials used were:

- *AlN*: Aluminum nitride was hot pressed into discs, 25 mm in diameter and 5 mm in thickness. The samples exhibited less than 3% open porosity and a thermal conductivity of about 80 W/m · K.
- *AM25*: This nomenclature refers to an AlN-Mo ceramic matrix composite containing 25% by volume of dispersed metallic phase. Sintering of these samples was performed at the laboratory under the same conditions as those employed for pure AlN. The samples exhibited less than 3% open porosity and a homogeneous microstructure.
- *FT25*: These substrates were disc shaped, 5 mm in thickness, cut from 25 mm diameter grey cast iron rods, and were employed to obtain complementary information about coating structure and properties, independent of the substrate nature.
- *Mo*: Molybdenum substrates were disc shaped, 25 mm in diameter and 5 mm in thickness, cut from dense molybdenum rods.

Table 1 presents the principal characteristics of the substrate materials.

4. Spraying of Coatings

Initial experiments were performed to study the formation of splats on polished substrates (surface roughness less than 0.1 μm). The spreading behavior of plasma-sprayed particles impinging on a flat substrate determines the shape and thickness of the splat as well as the real area of contact between the flattened droplet and the substrate surface. The contact area determines the coating cohesion and adhesion through parameters such as surface roughness, particle velocity, and molten state upon impact (Ref 11). The flattening behavior of molybdenum and tungsten powders on the substrates mentioned in section 3 was studied under varying preheating conditions. Splat observation

revealed that molybdenum particles present better spreading behavior on pure AlN substrates than tungsten particles. Only molybdenum particles remained adherent to all type of substrates, whereas tungsten particles adhered only to metallic substrates (FT25 and Mo). Compatibility studies undertaken (Ref 12-14) between Mo-AlN and W-AlN showed that molybdenum exhibited better bonding to AlN.

Grit blasting was employed to improve the surface roughness of substrates, and thereby to improve the mechanical adhesion of the coatings (Ref 15). The controlled parameters were the blasting time, pressure, and white alumina grit size (Ref 16) in order to obtain the appropriate surface roughness parameter (R_a). Grit blasting also helps to remove the preexisting thin ox-

Table 1 Principal characteristics of different substrate materials

Material	Specific mass, kg/m^3	Melting point, $^{\circ}\text{C}$	Thermal conductivity, $\text{W/m} \cdot \text{K}$	Coefficient of thermal expansion, $10^{-6}/\text{K}$	Young's modulus, GPa
AlN(a)	3260	2450(b)	80	6.84 (1500 K)	313
AM25(a)	4900	≈ 2450 (b)	105	7.6 (1500 K)	323
FT25	7200	≈ 1350	30	11 (1000 K)	200
Mo	10,200	2625	138	7.58 (1500 K)	322
W(c)	19,300	3410	173	5.08 (1500 K)	400

(a) Values given were measured in the laboratory. (b) Decomposition. (c) Values given for comparison

Table 2 Optimized grit blasting values for different substrates

Material	Blasting pressure, Pa	Blasting time, s	Particle size, μm	R_a , μm
AlN	2×10^5	3	400	3.33
AM25	4×10^5	3	400	2.7
FT25	4×10^5	3	400	3.6
Mo	4×10^5	3	400	3.2

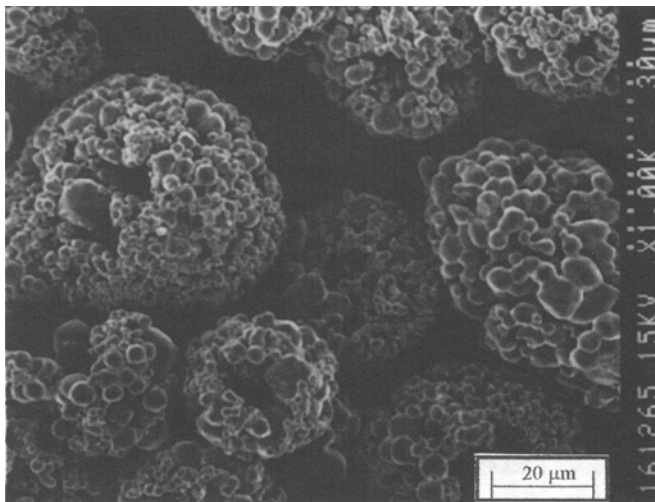


Fig. 2 Structure and shape of molybdenum powder

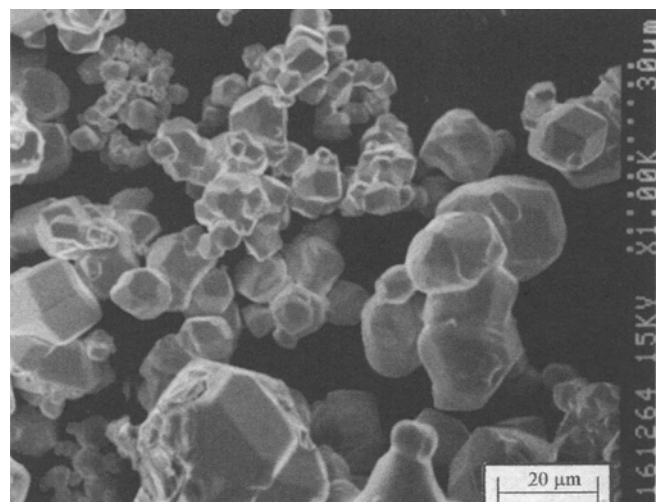


Fig. 3 Structure and shape of tungsten powder

ide layer from the substrate surface. Ultrasonic cleaning in acetone was performed after the grit blasting to remove the embedded grit particles and impurities from the surface. The surface state was characterized by using a surface profilometer Dektak II A and an optical microscope Olympus PMG 3 equipped with an image analysis facility. Table 2 gives the values of pressure, blasting time and white alumina particle size for which the substrate R_a was between 2.7 and 3.6 μm . Blasting distance was kept at 120 mm. Pressures higher than 4×10^5 Pa were found to be capable of provoking fracture, notably of the pure AlN substrates.

Plasma spraying was performed under low-pressure argon atmosphere ($\approx 5 \times 10^4$ Pa). An initial vacuum of 100 Pa was attained in the spraying chamber before the introduction of argon gas. Preheating of the substrate was carried out with the help of the plasma jet, and the temperature evolution was measured using a bichromatic pyrometer Ircon Mirage series OR (Ircon, Inc., Niles, IL) whose wavelengths were 0.7 and 1.08 μm , respectively. This type of pyrometer is sensitive toward the variation of intensity ratio between the two wavelengths, and it can thus tolerate small objects in its vision field, such as dust particles, as long as these objects affect the intensities corresponding to these two wavelengths in the same manner.

4.1 Molybdenum Coatings

Table 3 presents the parameters used in the spraying of molybdenum on AlN, AM25, FT25, and molybdenum substrates. The sample preheating was performed with a plasma jet for a period of 120 s. The samples were cooled down to the ambient temperature after the spraying operation, in the spraying chamber, under conditions similar to those used during spraying in order to minimize quenching and to avoid any chemical reactions with the air atmosphere. The samples were cut with a high-speed diamond cutting wheel and polished. Rough polishing was done with SiC papers starting from grade 500 and finishing with grade 1200, for 15 min each. Fine polishing was performed using diamond pastes of 6, 3, and finally 1 μm . A nonaqueous lubricant (Struers DP red) was used for the fine polishing, which prevented contamination of the metallic coating and substrate. The morphology of the films was studied by optical and scanning electron microscopy, and finally the adhesion tests were performed on the uncut samples in accordance with DIN 15160 B, a German standard.

Table 3 Parameters used for spraying coatings on AlN, Mo, AM25, and FT25 substrates

Parameter	Mo coating	W coating
Spray time, s	270	250
Powder flow rate, kg/h	1.8	1.8
Current, A	700	685
Voltage, V	64	67
Distance, mm	100	100
Argon flow rate, slm	45	45
Hydrogen flow rate, slm	15	15
Preheating temperature, °C	400	600
Carrier gas	Ar	Ar
Carrier gas flow rate, slm	4.8-5	5.5-6

4.1.1 Coating and Interface Microstructures

A micrograph of the interface between the molybdenum coating and AM25 substrate is shown in Fig. 4. The substrate is composed of molybdenum particles dispersed within an AlN matrix. The interface is regular and exhibits some porosity. It can also be observed that the molybdenum particles of the AM25 substrate, which are at the interface, are completely fused to the coating, thus improving the adhesion between the coating and the substrate. This result is supported by the adhesion measurements presented in the later part of this section. The coating shows a lamellar structure (Fig. 5) with an interlamellar open porosity, obtained through a density measurement, of about 17%. Coating thickness appears to be uniform, measured around 250 μm for the spraying conditions given in Table 3. The coating is composed of thin splats (~ 5 μm) and pores (~ 1.5 μm) that form a regular discontinuity within the structure. As discussed in section 3, concerning the molybdenum powder parti-

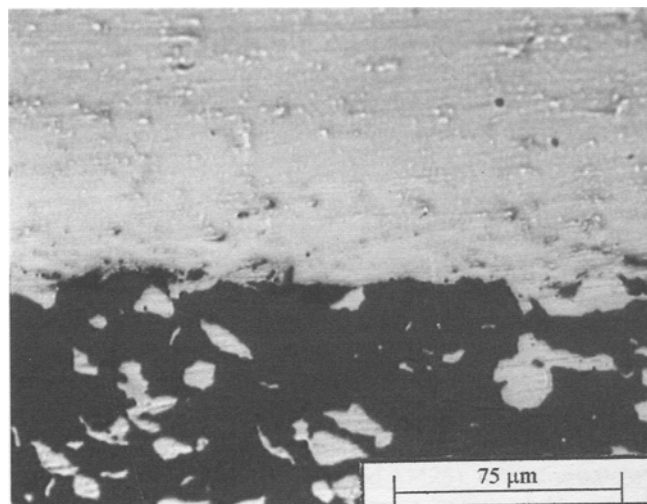


Fig. 4 Scanning electron micrograph of the interface between molybdenum coating and AM25 substrate

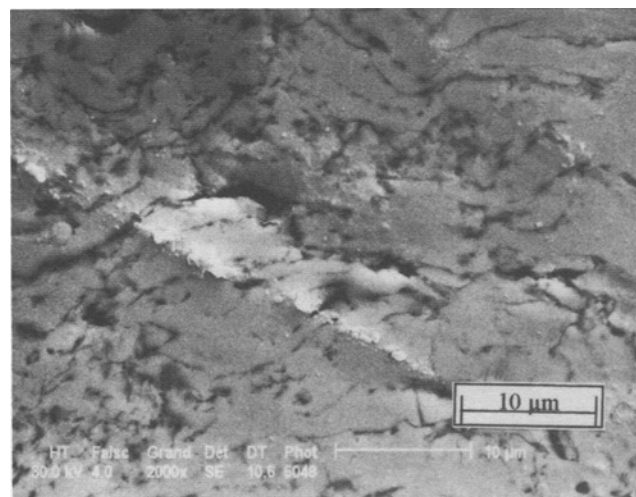


Fig. 5 Scanning electron micrograph of molybdenum coating, showing its lamellar structure and porosity

cles, this thin splat size probably results from particle breakdown during spraying.

4.1.2 Adhesion Measurements

The coated disc-shaped samples, 25 mm in diameter and 5 mm in thickness, were glued between two traction heads. A thermosetting glue (Araldite) was applied between the two surfaces. This glue, when heated for 3 h at 180 °C, exhibits a tensile strength of almost 60 MPa. The measurement was performed at a cross-head speed of 0.1 mm/min and the results have 10% error.

Table 4 shows that molybdenum coatings exhibit good adhesion on metallic substrates (molybdenum and FT25), with mean values of the tensile strength being 43 and 40 MPa, respectively, whereas this value is poor when the substrate is pure aluminum nitride (~3.5 MPa). The adhesion on AM25 gives an intermediate value (~11.5 MPa). After observation of the interface (Fig. 4) it becomes clear that adhesion is mainly provided by the molybdenum grains present at the AM25 surface. This reasoning correlates well with the area fraction of molybdenum particles at the surface of AM25 (i.e., the couple Mo-AM25 gives an adhesion value which is almost four times smaller than the value obtained for the Mo-Mo couple, because only about 0.25 of the surface fraction of AM25 is covered with molybdenum grains).

4.2 Tungsten Coatings

Table 3 summarizes the spraying parameters employed to spray tungsten coatings on AlN, AM25, FT25, and molybdenum

Table 4 Mean values of tensile stress required to remove molybdenum coatings from different substrates

Substrate	Strength, MPa
Mo	43 ± 4
FT25	40 ± 4
AM25	11.5 ± 1.5
AlN	3.5 ± 0.5

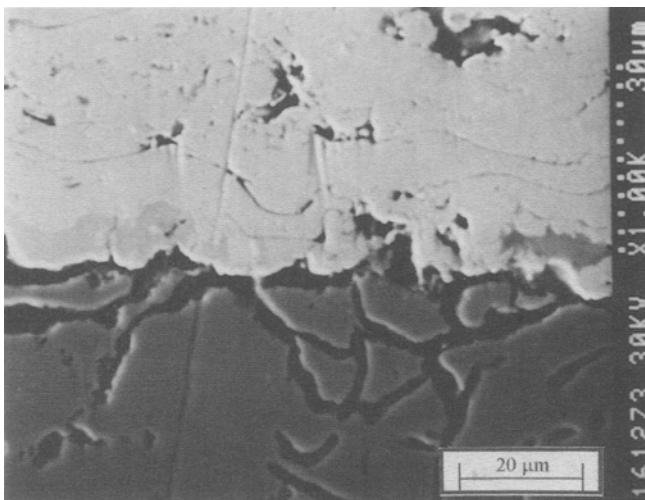


Fig. 6 Scanning electron micrograph of the interface between tungsten coating and FT25 substrate

substrates. The powder characteristics given in section 3 show that tungsten powder presents a wider size distribution range compared to that of molybdenum (−45 to +5 μm for tungsten and −45 to +10 μm for molybdenum) and that the tungsten powder particles are not spray dried and sintered agglomerates, as is the case with molybdenum powder, but are solid grains of different sizes sintered together to form larger agglomerates. This powder also contains an important amount of fine particles formed by deagglomeration, probably resulting from incomplete surface melting during sintering.

The substrates were preheated to 600 °C, which corresponds to a 4 min preheating time, under an argon atmosphere, with the plasma jet. A relatively higher carrier gas flow rate of about 6 slm was used, despite the higher density of the tungsten powder, which normally would require a lower carrier gas flow rate, in order to adjust for the finer particles in the tungsten powder and a wider size distribution range. After spraying, the samples were cooled to room temperature inside the chamber under argon atmosphere (5×10^4 Pa), in order to avoid any reactions at the coating surface. Samples were prepared for adhesion measurements or cut and polished to observe the coating structure and the interface.

4.2.1 Coating and Interface Microstructures

Figure 6 shows the interface between tungsten coating and FT25 substrate. The coating shows a lamellar structure with a small amount of open porosity that varies between 10 to 12%. The difference in the powder particle shape, structure, and size distribution seems to be an important factor responsible for such variation between molybdenum and tungsten coating microstructure and density.

4.2.2 Adhesion Measurement

Table 5 gives the values of tensile stress required to remove tungsten coatings from the surfaces of different substrates. It can be seen that tungsten does not adhere to AlN and AM25, but exhibits good adhesion to molybdenum and FT25. This finding indicates that the best way to obtain a tungsten coating on AM25 substrates is to use an underlayer of molybdenum between the coating and the substrate.

5. Discussion

The nature and structure of the feedstock plays an important role in determining the characteristics of sprayed coatings. Molybdenum powder was composed of quasispherical agglomerated and sintered particles obtained through the spray drying process. These agglomerates appeared to be hollow and partially sintered. This type of powder structure is susceptible to breakdown during spraying due to its lower mechanical strength. Tungsten powder was composed of dense sintered agglomerates containing a relatively higher quantity of fine particles.

An important characteristic of spray powders, which (in addition to other characteristics) gives a good indication of the powder behavior during plasma spraying, is the amount of heat required by a given mass of powder to bring it from room temperature to the molten state. This value, $m \cdot c_p \cdot \Delta T + m \cdot L_f$,

where c_p , L_f , m , and ΔT are the specific heat, latent heat of fusion, mass of the material, and the temperature difference between the sample temperature and its melting point, respectively, is higher in the case of molybdenum (951 J/g) than tungsten (631 J/g), although tungsten has the higher melting point (3410 °C for tungsten against 2610 °C for molybdenum). Tungsten has a higher thermal conductivity compared to molybdenum (173 W/m · K for tungsten against 138 W/m · K for molybdenum), and the amount of energy required to melt a given mass of tungsten is lower than that required for molybdenum. These factors indicate that tungsten powder particles attain their molten state during spraying more rapidly than molybdenum.

These differences in the powder properties allow differences in the observed coating microstructure to be understood. Tungsten coatings exhibit low open porosity (<12%) with thicker splats (Fig. 7), which results from adequate melting of individual particles. Molybdenum coatings show a higher porosity (~17%) and a thin lamellar structure (Fig. 5). This probably is the result of particle breakdown and incomplete melting of fine particles during spraying. Another important phenomenon could be the fact that lighter molybdenum particles show a tendency to remain at the plasma jet periphery, which is a low-temperature zone.

6. Conclusions

The objective of this study was to obtain tungsten coatings on AlN-Mo ceramic matrix composites, for their possible use as

Table 5 Mean values of tensile stresses required to remove tungsten coatings from different substrates

Substrate	Strength, MPa
Mo	41 ± 4
FT25	36 ± 4
AM25	...
AlN	...

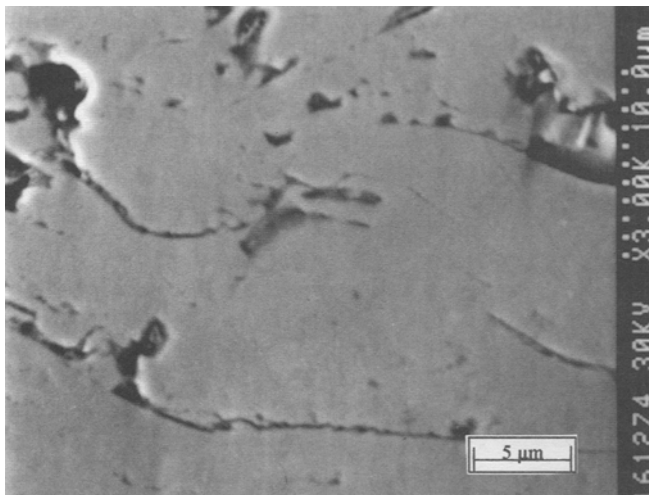


Fig. 7 Scanning electron micrograph of tungsten coating, showing its lamellar structure and porosity

substrates in high-power x-ray tube anodes. These tungsten coatings serve as targets and need to be deposited on an appropriate support material. Spraying was performed using the low-pressure plasma spraying technique under an argon atmosphere, which presents a number of advantages over the atmospheric plasma spraying technique.

Preliminary studies concerning grit blasting and splat formation were undertaken that allowed the spray parameters to be fixed. Spraying of molybdenum and tungsten coatings was performed on different metal, ceramic, and composite substrates. Molybdenum coatings were studied in view of their possible application as an under-layer. The results are summarized as follows:

- Molybdenum coatings exhibited a fine homogeneous lamellar structure with almost 17% open porosity. The splats forming the coating were small (~5 μm) compared to the powder particle size (10 to 45 μm). This could be due to the fact that powder particles, which were in the form of spherical hollow sintered agglomerates, break down during the spraying process.
- Molybdenum coatings showed good adhesion to the metallic substrates (molybdenum and FT25) with mean values of 43 and 40 MPa, respectively, whereas weak adhesion was observed on pure AlN substrate (3.5 MPa). An intermediate value of 11.5 MPa was found for molybdenum coatings over AM25 substrates, corresponding roughly to the 25% Mo at the surface of the AM25 composite material.
- Tungsten coatings showed a relatively thicker lamellar structure with a porosity content varying between 10 and 12%. This difference in structure, compared to that of the molybdenum coatings, could be attributed to the difference in powder particle nature, structure, and size distribution.
- No adhesion was observed between tungsten coatings and nonmetallic substrates (AlN and AM25). Adhesion on molybdenum and FT25 showed mean values of 41 and 36 MPa, respectively. The use of a molybdenum under-layer appears to be mandatory to obtain tungsten coatings on an AM25 substrate.

References

1. A.A. Khan, "Elaboration and Characterization of a Ceramic-Metal Composite, Used as a Substrate for High Power X-Ray Tube Anodes," Ph.D. dissertation, University of Limoges, 1995
2. P.C. Wolf and F.N. Longo, Vacuum Plasma Spray Process and Coatings, *General Aspects of Thermal Spraying: Proc. Ninth Int. Therm. Spray. Conf.*, J.H. Zaat, Ed., Nederlands Instituut voor Lastechniek, 1980, p 187-196
3. K.D. Borbeck, Robotics and Manipulators for Automated Plasma Spraying and Vacuum Plasma Spraying, *Proc. Tenth Int. Therm. Spray. Conf.*, DVS Düsseldorf, 1983, p 99-104
4. D.J. Varacalle, L.B. Lundberg, M.J. Jacox, J.R. Hartenstine, W.L. Riggs, H. Herman, and G.A. Bancke, Fabrication of Tungsten Coatings and Monolithics Using the Vacuum Plasma Spray Process, *Surf. Coat. Technol.*, Vol 61, 1993, p 79-85
5. R.W. Smith and M. Mohanty, Lightweight TiC/Ti Alloy Wear Resistant Coatings for Lightweight Materials in Aerospace Applications, *Thermal Spray Industrial Applications*, C.C. Berndt and S. Sampath, Ed., ASM International, 1994, p 73-77
6. P. Siitonen, T. Konos, and P.O. Kettunen, Corrosion Properties of Stainless Steel Coatings Made by Different Methods of Thermal Spraying,

- Thermal Spray Industrial Applications*, C.C. Berndt and S. Sampath, Ed., ASM International, 1994, p 105-110
7. C. Moreau, S. Boire-Lavigne, and R.G. Saint-Jacques, The Relationship between the Microstructure and Thermal Diffusivity of Plasma Sprayed Tungsten Coatings, *Thermal Spray Industrial Applications*, C.C. Berndt and S. Sampath, Ed., ASM International, 1994, p 621-626
 8. X.L. Jiang, R. Tiwari, F. Gitzhofer, and M.I. Boulos, Plasma Deposition of Refractory Metals, *Thermal Spray Coatings: Research Design and Applications*, C.C. Berndt and T.F. Bernecki, Ed., ASM International, 1993, p 309-313
 9. T. McKechnie, P. Krotz, Y.K. Liaw, F. Zimmerman, R. Holmes, and R.M. Poorman, VPS Forming of Refractory Metals and Ceramics for Space Furnace Containment Cartridges, *Thermal Spray Coatings: Research Design and Applications*, C.C. Berndt and T.F. Bernecki, Ed., ASM International, 1993, p 297-301
 10. S. Sampath and S.F. Wayne, Plasma Sprayed Mo-Mo₂C Composites: Microstructure and Properties, *Thermal Spray Coatings: Research Design and Applications*, C.C. Berndt and T.F. Bernecki, Ed., ASM International, 1993, p 397-403
 11. S. Fantassi, M. Vardelle, A. Vardelle, and P. Fauchais, Influence of the Velocity of Plasma Sprayed Particles on the Splat Formation, *Thermal Spray Coatings: Research Design and Applications*, C.C. Berndt and T.F. Bernecki, Ed., ASM International, 1993, p 1-6
 12. P. LeFort and R. Queriaud, Compatibility between Molybdenum and Aluminium Nitride, *J. Eur. Ceram. Soc.*, Vol 13, 1994, p 329-333
 13. R. Queriaud, P. LeFort, and M. Billy, The Direct Bonding between AlN Ceramics and CaO Doped Tungsten, *J. Eur. Ceram. Soc.*, Vol 8, 1991, p 319-325
 14. P. Denoirjean-Deriu and P. LeFort, Evolution of the Secondary Phase AlON in AlN during Its Bonding with CaO Doped Tungsten, *J. Eur. Ceram. Soc.*, Vol 11, 1993, p 359-362
 15. A. Tronche and P. Fauchais, Hard Coatings (Cr₂O₃, WC-Co) Properties on Aluminium or Steel Substrates, *Mater. Sci. Eng.*, Vol 92, 1987, p 133-144
 16. M. Mellali, A. Grimaud, and P. Fauchais, Parameters Controlling the Sand Blasting of Substrates for Plasma Spraying, *Thermal Spray Industrial Applications*, C.C. Berndt and S. Sampath, Ed., ASM International, 1994, p 227-232